

# A Three-Stage Cascaded Staggered Double Vane for a 220 GHz Traveling-Wave Tube

Guangsheng DENG, Xiaoling HUANG, Jun YANG, Zhiping YIN and Jiufu RUAN

Academy of Opto-Electronic Technology, Hefei University of Technology, Hefei, 230009, China

(Received 16 June 2015 / Accepted 12 August 2015)

This paper presents a simulation of a three-stage cascaded staggered double vane slow-wave structure (SWS). The results suggest that  $>10$  W of peak power can be produced between 208 GHz and 238 GHz and a maximum gain of 32.4 dB at 220 GHz, driven by three 20 mA electron beams. The proposed circuit does not require an attenuator and the length of each stage is 27.45 mm. Because of the current density and short circuit length, the structure shows application potential as a terahertz radiation source.

© 2015 The Japan Society of Plasma Science and Nuclear Fusion Research

Keywords: multi-beam, cascaded amplifier, staggered double vane (SDV), slow-wave structure (SWS)

DOI: 10.1585/pfr.10.1406078

## 1. Introduction

Because of advances in fabrication and device physics modeling [1, 2], the interest in new, practical sources of terahertz (THz) vacuum electronic devices (VEDs) has recently resurged. The traveling-wave tube (TWT) is one of the most important terahertz wave vacuum amplifiers because of its outstanding bandwidth and power capacity. Some 0.22-THz TWTs for the atmospheric window have been developed [3, 4], which have also been investigated recently [5, 6]. Paoloni and Mineo [7] studied a TWT based on the double corrugated waveguide. Hou *et al.* [8] proposed a novel slow-wave structure (SWS) called ridge-vane-loaded folded waveguide. Xu *et al.* [9] and Shin *et al.* [10] presented a THz TWT based on a sine waveguide and staggered double vane (SDV), respectively. Most of the THz TWTs require relatively long circuit lengths; however, fabrication issues, beam interception, and electron beam thermal effects dominate and ultimately limit the circuit length in practice. Moreover, the fabrication of tiny concentrated attenuators, necessary for high-gain THz TWTs, is challenging.

Nguyen *et al.* [11] presented a TWT based on a three-stage cascaded folded waveguide with every stage connected end-to-end and the RF carrying information between the stages. In this structure, the circuit length is significantly reduced. Based on this idea, we propose a three-stage cascaded SDV TWT with the advantages of the cascaded folded waveguide TWT. Moreover, in such a cascaded SDV TWT, only a 20 mA beam current is required at each stage. Compared with the cascaded folded waveguide TWT having the same output power, the beam current in our proposed TWT is 20% lower, offering significant improvements in beam generation and focusing.

## 2. Model and Transmission Characteristics

The 3D single cell of the SDV SWS is shown in Fig. 1, together with the dispersion curve of the fundamental mode under the first spatial harmonic operation based on the CST eigenmode calculation. The normalized phase velocity is given by

$$v_{\text{Nor}} = v_p/c, \quad (1)$$

where  $v_p$  is the phase velocity of the fundamental mode under the first spatial harmonic, and  $c$  is the speed of light.

In the SWS of a TWT, the interaction impedance of the first spatial harmonic is given by

$$k_c = \frac{|E_z|^2}{2\beta^2 P_w}, \quad (2)$$

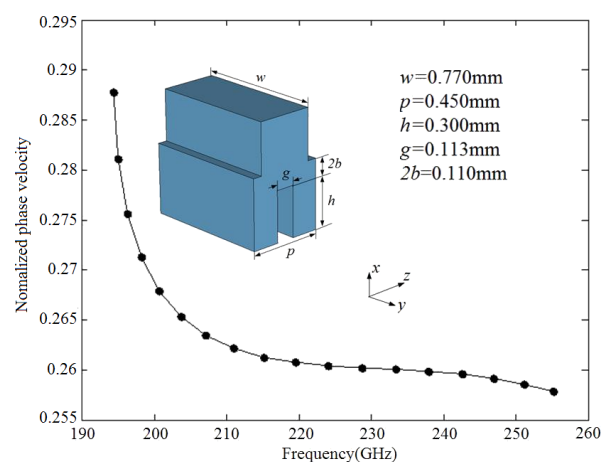


Fig. 1 Dispersion curve of the fundamental mode under the first spatial harmonic of the SWS. The insert shows the single-cell 3D schematic of the SWS with geometric parameters.

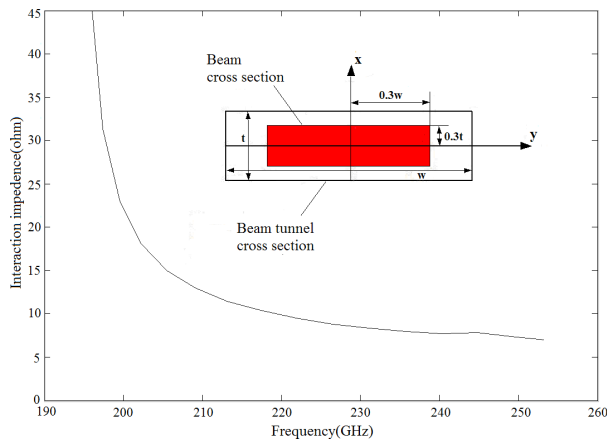


Fig. 2 Average interaction impedance of the SWS. The insert shows the beam cross section and beam tunnel cross section.

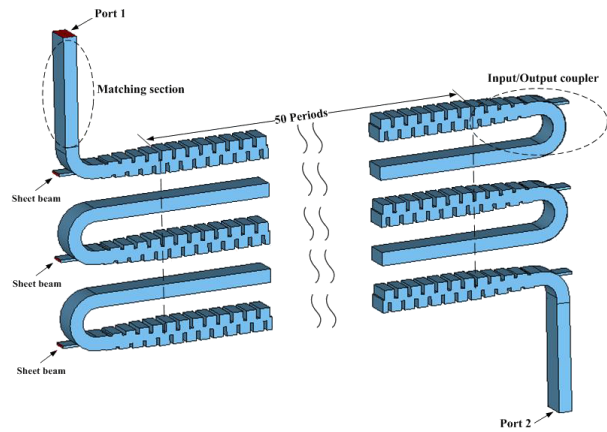


Fig. 3 Three-dimensional model of the three-stage cascaded SDV SWS.

where  $P_w$  is the electromagnetic wave power along the axial direction, and  $E_z$  and  $\beta$  are the amplitudes of the axial component of the electric field and the phase constant of the first spatial harmonic, respectively. The effectiveness of beam–wave interaction depends on the average interaction impedance over the cross section of the beam; thus, 400 points uniformly distributed on the beam cross section were used in the calculation, as shown in Fig. 2. At lower frequencies, the interaction impedance is relatively high, the phase velocity varies drastically, and synchronization of the electron beam and electromagnetic wave is difficult. As frequency increases, the dispersion and interaction impedance curves flatten; therefore, the beam–wave interaction stabilizes at high frequencies.

Figure 3 shows the three-stage cascaded SDV SWS model. The three-stage structure is adopted to reduce the circuit length in each stage and to increase the output power. Each stage is connected by a straight waveguide and an input–output coupler that comprises the transition structure of the SWS and an input–output connector. The end of the third stage is at the axial position, where

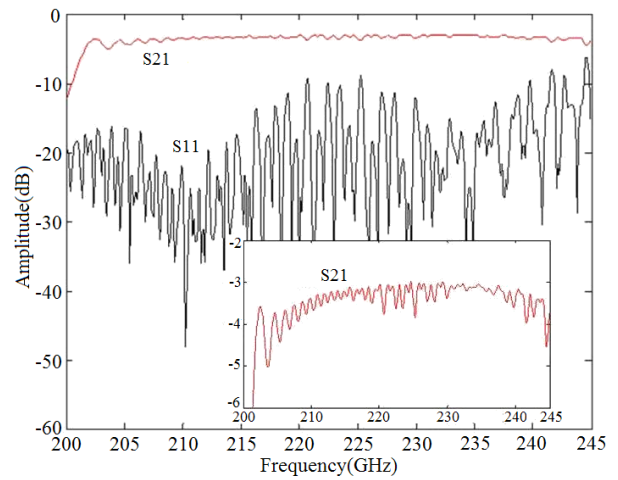


Fig. 4 S parameters of the model. The lower right inset shows details of the S21 curve.

the power starts to decrease because of saturation to verify the maximum output power. Considering the small size of the three-stage cascaded SDV SWS, the whole structure was manufactured by UV-LIGA with a tolerance of  $<2 \mu\text{m}$  for each cell. A five-period tapered staggered double vane was used as the transition structure and a semicircular arc-shaped waveguide was used as the input–output connector. A matching section was also included in the structure to connect the WR-3 standard waveguide to Port 1 or Port 2.

The signal transmission characteristics of the model were analyzed with the CST transient solver. In all calculations, we assumed that the structure material was oxygen-free high-conductivity copper with a conductivity of  $5.8 \times 10^7 \text{ S/m}$ . Figure 4 shows the signal transmission characteristics of the model in Fig. 3. The transmission losses S21 greater than  $-4 \text{ dB}$  and reflection parameter S11 less than  $-10 \text{ dB}$  are observed between 210 GHz and 240 GHz. The simulation results show that there is a moderate match from Port 1 toward Port 2 over the entire active band for the three-stage cascaded SDV SWS structure. Note that if we consider the surface roughness of the metal, the electrical conductivity of copper decreases to  $4.7 \times 10^7 \text{ S/m}$  according to [12]; thus S21 is approximately 1 dB lower than that in Fig. 4, which shows a  $<10\%$  decrease in the output power for the three-stage SDV SWS.

### 3. Interaction Results and Analysis

To investigate the amplification performance of the model, we used the PIC solver in the CST Particle Studio. In the simulation, each stage is driven by a 20 mA, 18.7 kV electron beam with an area of  $0.462 \times 0.066 \text{ mm}^2$ . The optimized height and width of the electron beam are 0.6 times those of the tunnel. A uniform longitudinal magnetic field of 0.3 T generated by a solenoid is used to guide the sheet electron beam. The axial electron velocity is about 1.05 times the phase velocity as the beam–wave interaction approaches maximum. A driving signal with a peak input

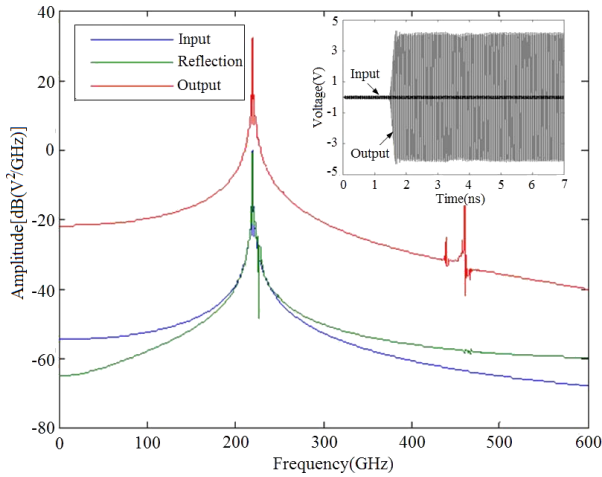


Fig. 5 Frequency spectrum of the input, output, and reflected signals of 220 GHz. The upper-right inset figure shows the input signal and the PIC simulation results of the output signals at 220 GHz.

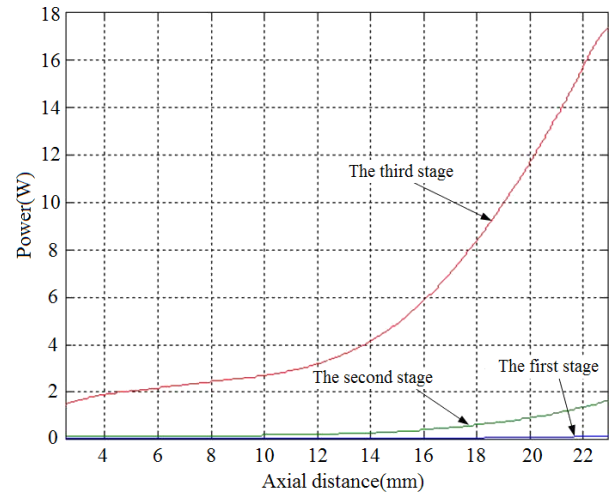


Fig. 6 Axial power distribution of the SWS at 220 GHz, where the input–output coupler and transition sections are not included.

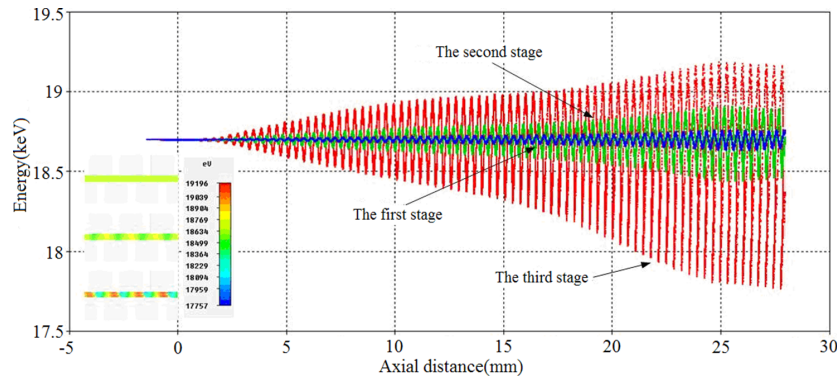


Fig. 7 Stable phase space plot of the bunched electron beam at 6 ns.

power of 10 mW was used in the simulation. For a single frequency, the simulation time was about 48 h with a 3.6 GHz processor.

The typical simulation results at 220 GHz are shown in Fig. 5. The output signal stabilizes at 17.6 W after 1.8 ns interaction until the end of the simulation time (7 ns). Figure 5 shows the frequency spectrum of the input, output, and reflected signals. The highly monochromatic amplified output signal peaks at 220 GHz and is 32.4 dB higher than the input signal. Oscillation was not observed. The gain increases with an increasing interaction impedance and beam current, and decreases with an increasing beam voltage.

The longitudinal power flow shown in Fig. 6 gives the RF power contributed by each stage; the maximum RF power and gain in each stage are 0.16 W, 1.77 W, 17.6 W and 12 dB, 10.4 dB, 10 dB, respectively. The criterion equation used to evaluate the stability of a tube is proposed in Ref. [13].

$$Q = G - L - \rho_o - \rho_i, \quad (3)$$

where  $G$  is the gain of the TWT,  $L$  is the circuit loss, and  $\rho_o$

and  $\rho_i$  are the reflection coefficients at the output and input, respectively. All four parameters are expressed in decibels. The tube oscillates if  $Q > 0$ . For the three-stage cascaded SDV SWS without an attenuator, each stage can be regarded as a single TWT; thus, the relatively low gain of each stage cannot cause oscillations according to Ref. [3].

The beam–wave interaction at each stage is shown in Fig. 7, which shows the phase space plot of the bunched electron beam at 6 ns for a steady-state electron dynamic system. The energy conservation law holds true between the sum of wave energy and ohmic loss energy and the decrease in the electron beam energy. However, a numerical error of  $\sim 4\%$  in the energy conservation is inevitable. Together with the inset electron cluster diagram, Fig. 7 shows the beam–wave energy exchange. In the first two stages, the beam–wave interaction is relatively weak because of the low electromagnetic field intensity, which leads to a small energy exchange between the beam and the wave. In the last stage, the signal is enhanced by the first two stages and strongly interacts with the electron beam, absorbing energy from the beam and markedly decreasing the elec-

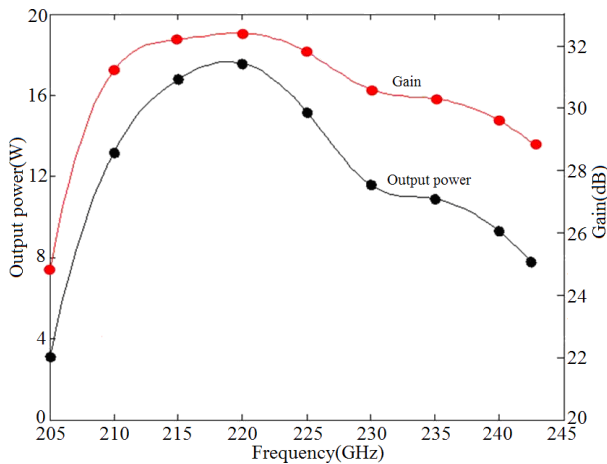


Fig. 8 Simulation results of the output power and total gain versus frequency of the TWT amplifier.

tron energy in the third stage.

The simulation results of the amplitude-frequency response are shown by plotting the output power versus the driving frequencies between 205 and 242 GHz, as shown in Fig. 8, in which the corresponding gain is also shown. The points are the simulation results and the lines are for visual aid. The power exceeds 10 W at frequencies  $> 30$  GHz with a maximum gain of 32.4 dB at 220 GHz. Considering the distribution of the electron energy from the electron gun, the output power will decrease at the central frequency and increase at the sides. However, the power decrease is higher at the central frequency and affected by the energy distribution of the electrons injected into the third stage.

#### 4. Conclusion

In summary, terahertz amplification in a three-stage cascaded SDV SWS has been demonstrated. An output power of 17.6 W with 32.4 dB gain at 220 GHz can be

achieved with a current density of  $62.5 \text{ A/cm}^2$  and a short circuit length of 27.45 mm. Moreover, a concentrated attenuator is not necessary in this structure. All these features make this compact all-in-one SWS a practical and promising terahertz radiation source.

#### Acknowledgments

This work was supported by the Fundamental Research Funds for the Central Universities under Grant JZ2015HGBZ0109.

- [1] J.X. Qiu, B. Levush, J. Pasour *et al.*, IEEE Microw. Mag. **10**, No.7, 38 (2009).
- [2] J.H. Booske, R.J. Dobbs, C.D. Joye *et al.*, IEEE Trans. Terahertz Sci. Technol. **1**, No.1, 54 (2011).
- [3] A. Baig, D. Gamzina, M. Johnson *et al.*, Experimental characterization of LIGA fabricated 0.22 THz TWT circuits, IVEC2011, 275 (2011).
- [4] N.M. Ryskin, A.G. Rozhnev, T.A. Karetnikova *et al.*, Modeling and characterization of a slow-wave structure for a sheet-beam sub-THz TWT amplifier, IVEC2013, 1 (2013).
- [5] Y.J. Wang, Z. Chen, Y.L. Cheng *et al.*, J. Infrared Millim. Waves **33**, No.1, 62 (2014).
- [6] H.R. Gong, G. Travish, J. Xu *et al.*, IEEE Trans. Electron Devices **60**, No.1, 482 (2013).
- [7] C. Paoloni and M. Mineo, 0.22 THz TWT based on the double corrugated waveguide, IVEC2014, 227 (2014).
- [8] Y. Hou, Y.B. Gong, J. Xu *et al.*, IEEE Trans. Electron Devices **60**, No.3, 1228 (2013).
- [9] X. Xu, Y.Y. Wei, F. Shen *et al.*, IEEE Electron Devices Letters **32**, No.8, 1152 (2011).
- [10] Y.M. Shin and L.R. Barnett, Appl. Phys. Lett. **92**, No.9, 091501 (2008).
- [11] K. Nguyen, L. Ludeking, J. Pasour *et al.*, Design of a high-gain wideband high-power 220-GHz multiple-beam Serpentine TWT, IVEC2010, 23 (2010).
- [12] E. Hammerstad and O. Jensen, Accurate Models for Microstrip Computer-Aided Design, Microwave Symposium Digest, IEEE MTT-S International (1980), p.407.
- [13] A.S. Gilmour, Jr., *Principles of Traveling-Wave Tubes* (Artech House, Boston, 1994).